JLAB-TN-06-048

Studies of Beam Halo Formation in the 12 GeV CEBAF Design

Yves Roblin and Arne Freyberger*

Beam halo formation in the 12 GeV beam transport design is investigated using beam transport models and data from 6 GeV operations. Beam halo due to beam gas scattering is shown to be less of a problem at the proposed higher energies than at 6 GeV. Beam halo due to non-linear effects of magnetic elements is characterized as a function of the beam orbit. For a beam orbit that is confined to less then ± 1 mm transverse of the nominal magnet center, the ratio beam halo to the beam core is less then 2.9×10^{-5}, where beam halo is defined as beam particles with at least ± 5 mm displacement from the beam center. The amount of beam halo as a function of the RMS beam orbit is presented.

Functional forms of the halo distribution are presented, these functional forms can be used to generate halo in subsequent studies and for detector optimization.

I. INTRODUCTION

There is not a widely accepted definition of beam halo as there are for other beam parameters. Understanding sources of halo generation is an active field with many sources of halo actively being researched [1]. In addition to the academic interest in beam halo, the experimental users of particle beams often have to deal with detector backgrounds which are generated by beam halo interactions. Large acceptance detectors are particularly sensitive to halo background since by their very nature (large acceptance) these detectors cannot easily discriminate between a beam-target interaction and a halo background interaction.

This note reports on studies of the transverse beam profile and halo generation in the CEBAF 12 GeV design. The study is motivated by the installation of a new large acceptance detector, glue$X$, in the new end-station D. Longitudinal beam halo is not an issue for the experimentalists and not part of this report. The rest of this introductory section formalizes the definitions used in this report and briefly summarizes the possible sources of halo. The next section describes the tools used to estimate the halo in the 12 GeV design. This is followed by a section the details the 12 GeV beam parameters used in the study. The results of the studies are then presented, followed by concluding remarks.

A. Halo Definition

The definition of the transverse halo used in this report is as follows. The core of the beam is described as a Gaussian distribution denoted as $\mathcal{G}(x)$ where x is the transverse dimension. The halo component is modeled by any arbitrary function, $\mathcal{H}(x)$. For some x, $\mathcal{G}(x) = \mathcal{H}(x)$, this value of x is denoted as x_{halo}. Halo is then defined as the ratio of the integrated particles from x_{halo} to the beam pipe radius to the area of the core Gaussian distribution;

$$H = \frac{\int_{x_{halo}}^{x_{pipe}} \mathcal{H}(x)dx + \int_{-x_{pipe}}^{-x_{halo}} \mathcal{H}(x)dx}{\int_{-x_{pipe}}^{x_{pipe}} \mathcal{G}(x)dx}. \tag{1}$$

While this definition is mathematically straight forward, the implications of beam halo depend not only on the value of H but also the value of x_{halo} and the functional form of $\mathcal{H}(x)$. Estimates of H, $\mathcal{H}(x)$ and x_{halo} are to be used in further studies to optimize the detector designs such that halo backgrounds are minimized.

B. Sources of Halo

Possible sources of beam halo in the 12 GeV design include, nonlinear elements, mismatched beam optics, and Coulomb scattering on the residual gas. Other possible sources which are not applicable to the 12 GeV design include space charge effects (12 GeV bunch charge is too small), beam-beam effects and other sundry sources that are specific to storage rings, colliding beams or high bunch charge beams.

*Electronic address: roblin@jlab.org, freyberg@jlab.org

Nonlinear Elements-Multipoles

The 12 GeV design incorporates the same lattice that is used in the 6 GeV CEBAF design/operation. Since the beam energy is doubled in the 12 GeV design yet the Arc radius is kept the same, the amount of synchrotron radiation is signifi cantly larger in the 12 GeV design then in the 6 GeV machine. While synchrotron radiation does not directly cause halo formation, it does cause emittance growth. The emittance growth results in larger beam sizes and this larger beam will sample the nonlinear magnetic fi elds (multipoles) more in the 12 GeV machine then are presently sampled in the 6 GeV machine.

In addition to the intrinsic beam size, the beam orbit displacement relative to the magnetic center contributes to the amount of multipole content the beam samples off the magnetic elements. The amount of sampling will depend on the RMS of the beam orbit centroid relative to the magnet center (design orbit). As the RMS of the beam orbit increases the beam halo will increase. It is not known what the functional form is for the amount of halo formation as a function of the magnitude of the RMS orbit.

Another mechanism that can change the amount of multipole sampling is mismatched beam optics. The result of a mismatched section of the transport is that the Twiss parameters are far from design values, which result in larger beam sizes yielding more sampling of the multipole content. For a well matched beam contributions from this source are negligible. The 12 GeV design requires that the beam be well matched to contain emittance growth and halo formation due to mismatched optics is estimated to be much smaller than other contributions.[2]

The effect of the multipoles is to distort the beam ellipse and accumulation of these nonlinear effects result in particles being pushed out of the nominal Gaussian distribution onto the tail of the distribution. In order to study halo formation, nonlinear particle tracking simulations must be used.

Beam Gas Scattering

Scattering off the electron beam off of any residual beam gas will form beam halo. There are several processes through which an electron interacts with the residual beam gas; elastic scattering off the nucleus, bremsstrahlung, and Møller scattering. Of these processes elastic scattering at small angles is the dominant process and is typically referred to as Mott scattering. When an beam electron elastic scatters off a beam gas atom, its energy is unchanged but its trajectory is slightly changed. A small angular change coupled with a large longitudinal distance leads to a transverse displacement. This transverse displacement will result in a tail on the transverse profi le.

The amount of beam halo due to residual beam gas scattering is proportional to the vacuum pressure in the beam pipe and the total pathlength of the beam. For the 12 GeV design the total pathlength is roughly 10% longer for the new end-station. The pressure in the beam pipe for the 12 GeV machine will be at the same level as the present operating machine. For a constant pressure and pathlength the amount of Mott scattering is proportional to $\frac{1}{E_{beam}^2}$. Therefore beam halo due to Mott scattering is expected to of order $\frac{1}{4}$ of the beam halo due to Mott scattering in the 6 GeV machine.

C. 6 GeV Experience

The sources of beam halo described above for the 12 GeV machine are present in the 6 GeV machine. How to scale the measured beam halo from the 6 GeV machine to the 12 GeV machine depends on the beam halo source. Scaling the beam halo due to multipole sampling is not clear, the 6 GeV beam is smaller (much less emittance dilution due to synchrotron radiation) but the beam orbit tolerance is 3 mm for the 6 GeV machine versus 1 mm for the 12 GeV machine. Scaling the beam halo due to Mott scattering is well understood. Information on the beam halo shape and symmetry between horizontal and vertical planes provides some guidance as to the source of the beam halo. Beam halo due to Mott scattering is azimuthal symmetric and will appear in both horizontal and vertical planes at the same level. Beam halo due to multipole sample need not be symmetric between horizontal or vertical planes.

During CEBAF operations measurement of the beam halo have been performed in the end-stations. The measurements of beam halo are performed with a wire scanner with a photomultiplier readout. The photomultiplier readout provides a large dynamic range. In the case of Hall-B, an integrating plate is used to extend the dynamic range even further[3]. The defi nition of beam halo in [3] is different than the one used in this document. Table I recasts the values found in [3] in terms defi ned in this note. The functional forms used to fi t the beam profi les [3] is the sum of two Gaussian functions, the values for the σ of the two Gaussians obtained in [3] are repeated here for completeness.

In addition to the Hall-B scans, large dynamic range scans using the same technique are performed in Hall-C. The result of one of these scans is shown in Figures 1 and 2. The beam halo is undetectable (hidden in the detector noise) in the X profi le and the Y profi le is quite distorted from a Gaussian shape. There is no observable halo on the X profi le, the upper limit on the amount of beam halo is $H < 10^{-5}$ at the 99% confi dence level. This is consistent with Hall-B results. The Y profi le is extremely

Scan	σ_{core} (mm)	σ_{halo} (mm)	x_{halo} (mm)	H
Dec5 X	0.045	0.380	0.22	2.3×10^{-5}
Dec9a X	0.053	0.470	0.28	6.1×10^{-6}
Dec9b X	0.052	0.494	0.28	4.6×10^{-6}
Dec9c X	0.052	0.476	0.28	4.1×10^{-6}
Dec5 Y	0.104	0.949	0.54	7.4×10^{-6}
Dec9a Y	0.110	0.855	0.59	2.3×10^{-6}
Dec9b Y	0.110	0.771	0.59	2.6×10^{-6}

Table I: Results for large dynamic range beam profile scans in Hall-B during 6 GeV operations. Beam current for these scans was a few nanoAmperes CW beam. The functional form for the beam halo $\mathcal{H}(x)$ is assumed to be a Gaussian with $\sigma = \sigma_{halo}$.

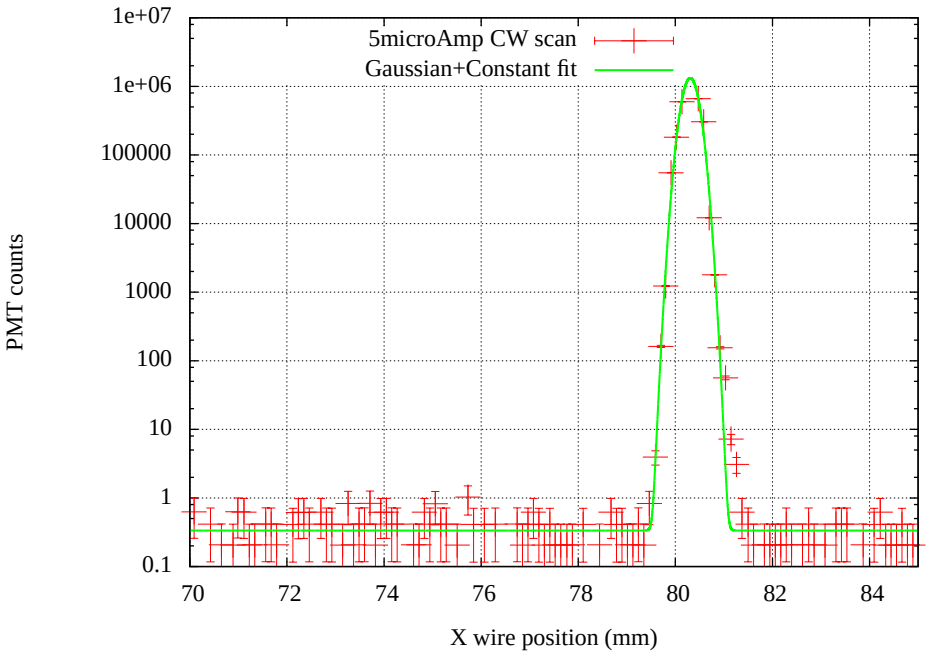

Figure 1: The horizontal beam profile in Hall-C. This profile was measured with 5μA of CW beam.

distorted and the distinction between beam halo and the distortion is not clear. For this reason determination of H for the Y profile is not presented.

II. METHODOLOGY

As previously stated the 6 GeV profiles and operational experience may not be directly applicable to the 12 GeV design. This is especially true for beam halo caused beam sampling the multipole content of the magnetic elements. In order to gain a better understanding of the expected beam halo in the 12 GeV design, the processes need to be simulated. If the beam halo in the 12 GeV design is of the same level as in the 6 GeV machine, the number of particles that must be simulated is at the order of 10^8 particles. Such large statistics are necessary in order to determine not only the level of halo, but also the functional form if it is at the 10^{-6} level.

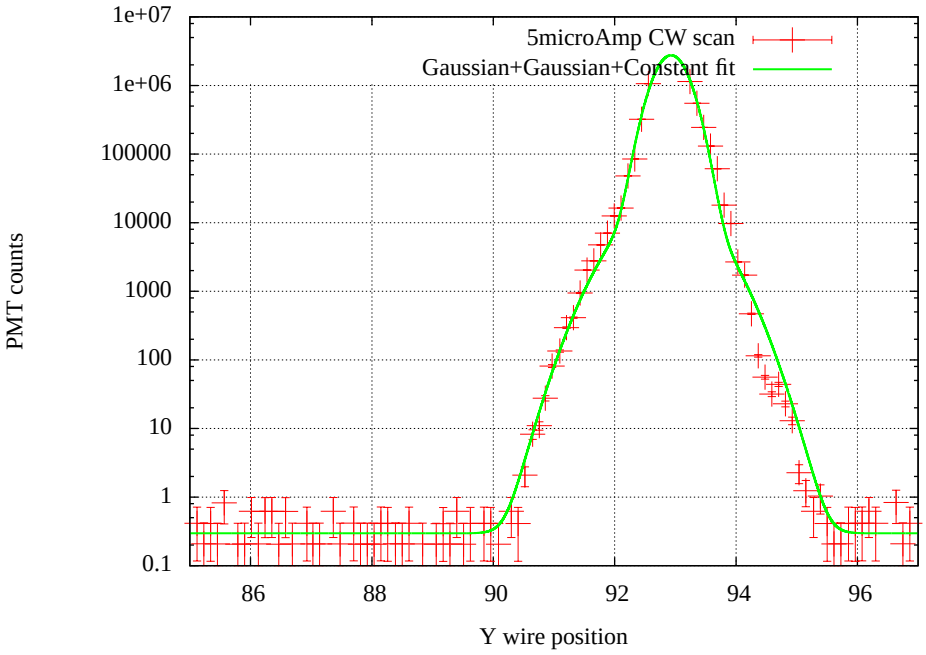

Figure 2: The vertical beam profile in Hall-C. This profile was measured with 5μA of CW beam.

A. Simulation Codes

DIMAD/Optim/Elegant

There are many accelerator codes available for simulating particle accelerators. Unfortunately CEBAF is a unique machine and most simulation codes are not applicable to the CEBAF design. For a realistic 12 GeV simulation the code must include synchrotron radiation effects, multipole effects, particle tracking that include non-linear effects and allow for large batch simulations. A survey of the available simulation codes suggested that `DIMAD` and `Elegant` have the feature set required for the 12 GeV design [4, 5]. Of the two, `DIMAD` is chosen as the primary simulation tool. `Elegant` serves as a check of linear issues as does `Optim`[6], and the bulk of the particle tracking is performed by `DIMAD`.

Each magnetic element is assigned multipole content. For those magnet types with measured multipole content, the measured multipole content is simulated. For magnet types with unmeasured multipole content, the amount of multipole content allowed by the the 12 GeV design requirements are simulated.

`DIMAD` does include software to simulate residual beam gas scattering [7]. These beam gas scattering routines were added to study residual gas scattering in storage rings (LEP). Verifi cation of the `DIMAD` treatment of beam gas scattering is of value as this is a recent addition to the software and there are other software packages that are specifi cally written to study particle interactions with material. This verifi cation is still on going and `DIMAD` will not be used to study beam gas scattering in this report.

GEANT4/g4beamline

Particle interactions with material is the domain of the `GEANT` family of particle codes. High energy and nuclear experimentalist use these codes to simulate particle interactions in the detector material. The software has a long tradition in the community and is well tested. The latest series of the `GEANT` software is version `GEANT4` [8]. `GEANT4` can be customized with upper level software, such a custom confi guration suitible for accelerator simulations has been developed [9]. `g4beamline` along with the underlying `GEANT4` program will be used to simulate the effects of residual beam gas scattering in the 12 GeV design.

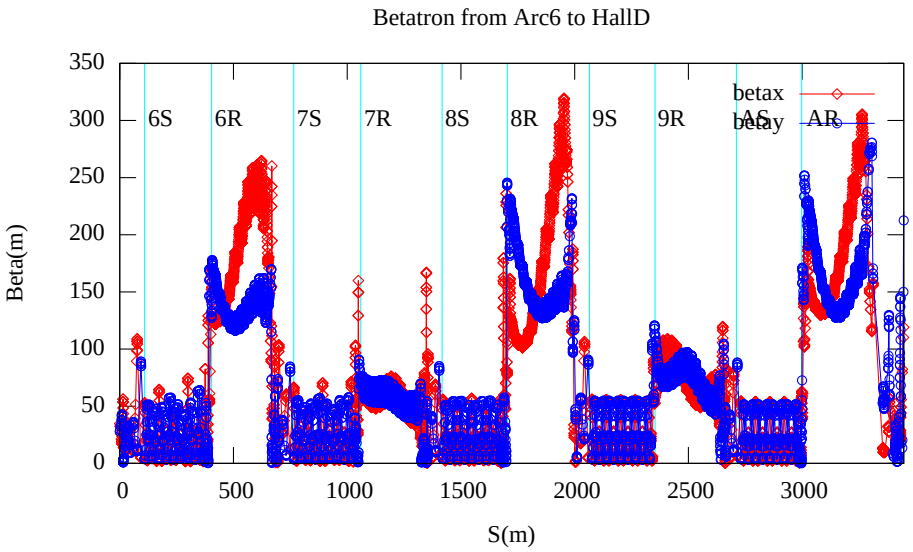

Figure 3: The betatrons for the 12 GeV lattice starting at 6S.

III. MODEL AND BEAM PARAMETERS

In order to study the effects of the multipoles on halo formation, we modeled the beam line from the entrance of the third pass southwest spreader (6S) to the hallD radiator target. The initial modeling was done in Optim and translated to DIMAD using an in-house tool. Cross-checks were performed to insure the integrity of the decks.

The synchrotron radiation becomes the main contributor to the emittance growth in the higher passes, starting around Arc6. As such, a tight control of the orbit and transport matching is required. The former places constraints on the steering tolerances and beam steering system design while the latter drives the level of magnet mispowering one can afford.

The beamline was instrumented with a set of correctors and beam position monitors whose location was chosen by borrowing from our experience with the current 6GeV machine.

The modeling started from the 6GeV machine and was modified to make it suitable for the 12GeV machine. A new arc (ARCA) was modeled for the extra half pass. The design was optimized for synchrotron radiation in higher passes by compromising the horizontal betatron amplitude in the lower passes in order to reduce it in the higher passes [13].

We used an hallD design with an 8 degrees bend for these simulations[11]. There is also a 10 degrees option which we did not use. As far as halo formation is concerned, the difference between the two decks is probably not significant since most of the halo induced by multipoles occurs over a long distance, along the entire machine, not just the last section in hallD.

The magnet apertures were set to their designed values (depending on the magnet type), while the beam pipe was modeled as elliptical collimators which are drifts with aperture restrictions.

After assembling the deck, the transport was matched at key locations, namely the start of each linac and entrance of each arc using the recombiner and spreader matching quadrupole magnets respectively. Finally, the beam was matched on the hallD radiator. An in-depth separate study was carried out to study the ability of the designed optics to absorb optical errors and correct the matching in presence of mispowering [10].

Finally transverse multipoles kick terms were added at the location of each dipole and quadrupole magnet. We used measured multipole values where available[14] and upper limits evaluated in a separate study by tracking where not[15].

A. Orbit Generation

In order to study the effect of multipoles on halo formation, we produced three orbits representative of a real machine.

Quadrupole magnets where randomly misaligned and mispowered and a global steering of the beamline was performed.

The monitor resolution chosen for the least square fit steering was adjusted to produce three orbits with standard deviations of 0.3 mm, 0.6 mm and 1 mm respectively. As can be seen from Figure 5, the corrector and monitor location is not optimized yet. Some spikes in the orbit mainly in the spreader and recombiners indicates inadequate coverage for proper steering. This issue as been explored elsewhere [12] and will not be covered in this note.

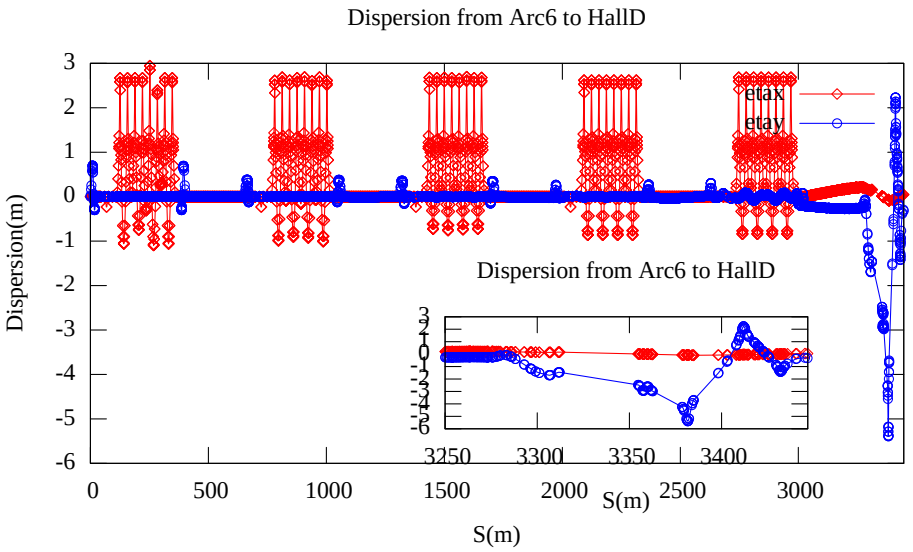

Figure 4: The dispersion functions for the 12 GeV lattice starting at 6S.

Three decks were produced with the same misalignments and resulting corrector settings to be used as starting point for the tracking studies.

B. Particle Tracking

The decks mentioned in the previous steps were modified to include a beam profile. This beam profile was defined by emittance and Twiss parameters taken from the design which took into account the synchrotron radiation growth. 5000 particles were generated and then tracked across the deck. This process was repeated 2000 times (with a different random seed every time) to yield 100 millions tracked particles. Tools were written to submit the DIMAD runs, analyze and accumulate the results in histograms of transverse beam profile at the location of the hallD radiator. Beam scraping information was also gathered by recording the location of each lost particle.

Most of the studies were performed on dual 2.66 GHz intel Xeon Linux workstations. Running 100 million particles for one orbit took about 180 hours on such machines.

IV. RESULTS

A. Multipoles

The transverse beam profile at the hallD radiator is given in figure 6 for 0.3mm, 0.6mm and 1mm sigma respectively and both transverse directions.

The profiles were fitted with a combination of Gaussian for the signal and a polynomial form for the background. The result of such fits is shown in figure 6. Tables II and III give the fitted parameters for the profiles. The first three parameters belong to the polynomial form: $\mathcal{H}(x) = p_0 + p_1 x^1 + p_2 x^2$ and the last three are defined for a Gaussian: $\mathcal{G}(x) = p_3 e^{-0.5\frac{(x-x_{mean})^2}{\sigma^2}}$.

$\sigma_{trajectory}$	p_0	p_1	p_2	p_3	x_{mean}	σ
0.3	2.95122e+01	4.18991	-2.39814e+05	3.53459e+06	-1.51249e-04	1.13205e-03
0.6	1.92730e+02	-4.54463e+02	-1.59354e+06	3.53125e+06	-3.78768e-04	1.13252e-03
1.0	5.95309e+02	-1.922347e+03	-4.97590e+06	3.52295e+06	-6.74874e-04	1.13281e-03

Table II: Value of fit parameters for background and core Gaussian for X profiles

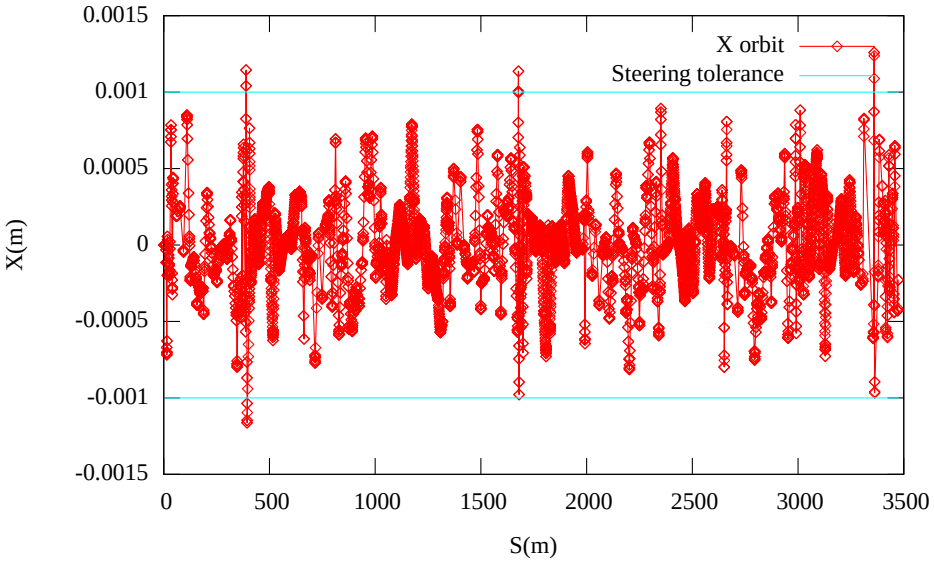

Figure 5: Transverse orbit with σ=0.3 mm

$\sigma_{trajectory}$	p_0	p_1	p_2	p_3	x_{mean}	σ
0.3	1.57989e+01	-1.05538e+03	-2.26489e+05	7.05901e+06	-1.06258e-03	5.66681e-4
0.6	5.27411e+01	-7.47562e+02	-6.21194e+05	7.06193e+06	-1.17167e-03	5.66261e-04
1.0	2.13733+02	-6.96938e+02	-2.09602e+06	7.05691e+06	-1.32710e-3	5.65706e-04

Table III: Value of fit parameters for background and core Gaussian for Y profiles

Integrating the background and the Gaussian form and forming the ratio as in equation (1) yields the results in Table IV

$\sigma_{trajectory}$ (mm)	N_{bg}	x_{halo} (mm)	H
0.3	1574	5.1	3.4×10^{-5}
0.6	6212	5.1	1.2×10^{-4}
1.0	15363	5.1	3.4×10^{-4}

Table IV: Value of ratio H for X orbits of various sigmas

B. Gas Scattering

Residual beam gas interactions via Mott scattering alter the beam angle but leave the beam energy unchanged. To study the effect of beam gas interactions, Geant4/g4beamline simulations were performed. A 400 m long drift is used to simulate the interactions through an Arc. A parallel beam with σ=100 μm and energy of 11 GeV is used to simulate the beam in the tenth Arc. Figure 7 shows the result for 1×10^{-7} through 1×10^{-6} torr of residual beam gas. A mixture of gasses resembling those in Air is used for the beam gas. At present the vacuum in the Arc region is not known, but thought to be $\leq 1\times10^{-7}$ torr. The amount of beam gas in the Linac sections is a few orders of magnitude less then in the Arcs (due to cryo-pumping of the super conducting cavities) and the simulations show that beam gas scattering at these pressures in negligible.

The background function, $\mathcal{H}(x)$, used to perform fits to the data is the sum of a Gaussian function and a constant term. The results of the fits and the derived value of H from these fits are shown in Table VI. While the data is very similar in shape to the Hall-B harp profiles (both are dominated by the sum of two Gaussians), the value for H is higher in the simulated data then that found in the 6 GeV measurements.

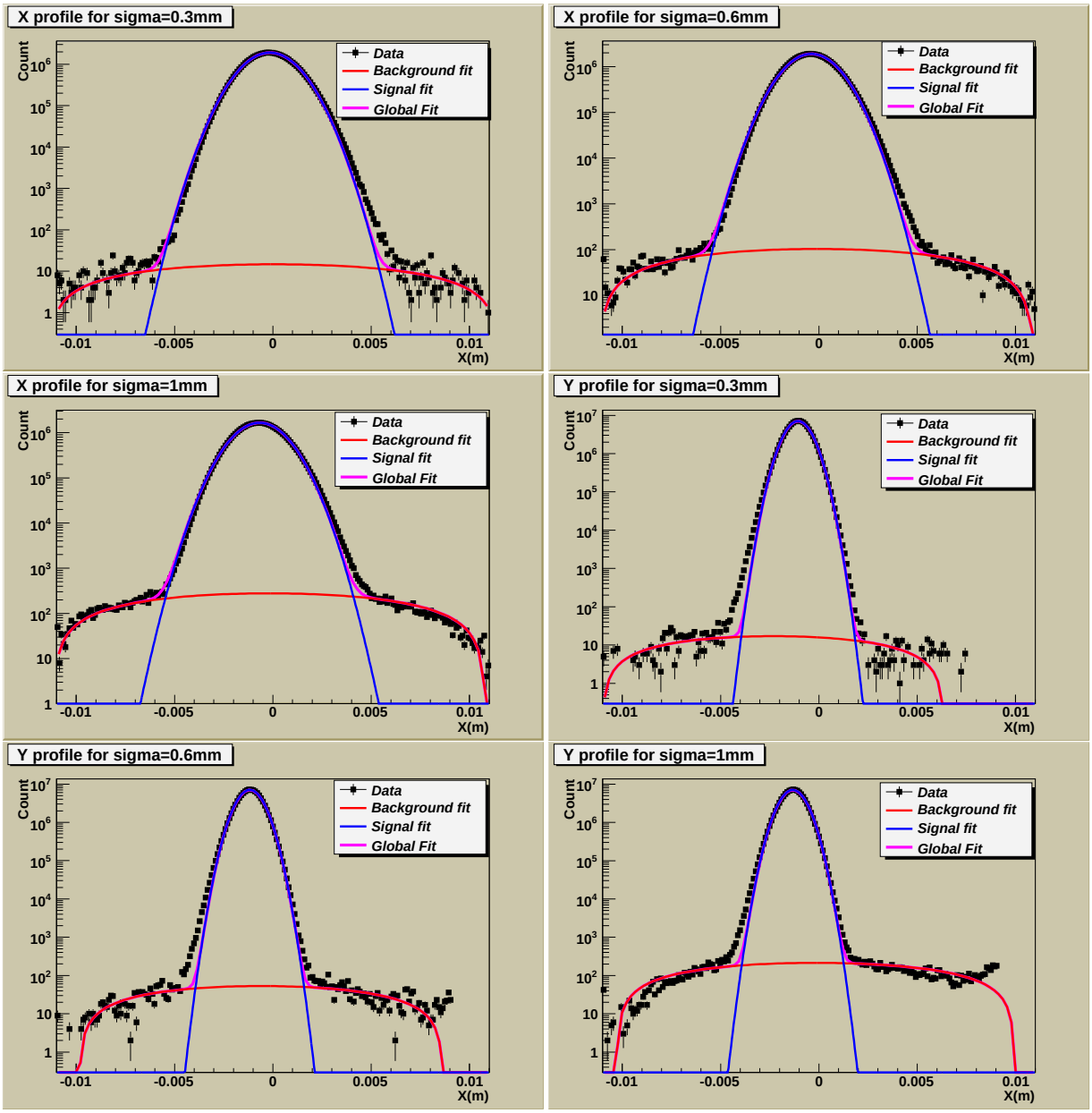

Figure 6: Background and signal fits

V. SUMMARY

The expected transverse beam profi le is an important beam quantity in the design of large acceptance spectrometers. Parameterization of the beam profi le through six or even seven orders of magnitude is needed to optimize the interface between the delivered beam and the experiment in terms of backgrounds from beam halo interactions. The sources of beam halo in the 12 GeV design include: non-linear effects due to multipole components and beam-gas interactions. Monte Carlo simulations of these effects in 12 GeV design have been performed.

Large 10^8 particle tracking simulation runs are used to study halo formation due to sampling of multipole components. These simulations are used to determine the amount of halo and its functional form. The amount of halo is found to depend on the quality of the central orbit. There is signifi cant reduction in the amount of halo as the RMS orbit is reduced from 1 mm to 0.3 mm. The functional form for the halo is well modeled by a polynomial of the second order.

The formation of beam halo due to residual gas scattering is expected to be a factor of 4 less at 12 GeV then at 6 GeV since the dominant process scales as $\frac{1}{E^2_{beam}}$. Experience with the large acceptance spectrometer in Hall-B shows that beam halo is not

$\sigma_{trajectory}$ (mm)	N_{bg}	x_{halo} (mm)	H
0.3	1044	3.1	1.0×10^{-5}
0.6	3822	3.1	3.8×10^{-5}
1.0	15153	3.1	1.5×10^{-4}

Table V: Value of ratio H for Y orbits of various sigmas

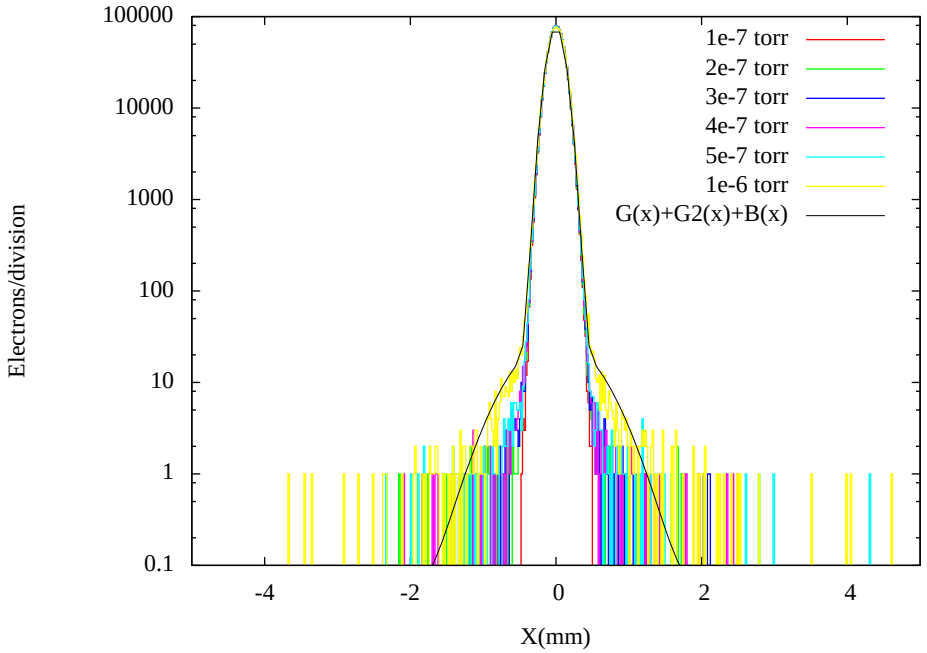

Figure 7: Transverse beam profile after traveling through 400 m of different residual beam gas pressures. The fit shown is for the 1×10^{-6} torr data.

a problem for the 6 GeV design. Nevertheless large statistics Monte Carlo simulations were performed. These simulations show the formation of beam halo with gas pressures as low as 2×10^{-7} torr. The functional form of the halo generating by beam gas scattering is observed to be different then that generated by the multipole components. While the Monte Carlo predicts the correct dependence on beam gas pressure, the amount of halo produced by this Monte Carlo is too large when comparisons are made with the 6 GeV data. Reconciling these issues is ongoing.

The results on the amount of halo and the functional form of the halo are to be used in the optimization the Hall-D detector.

Pressure (torr)	σ_{halo} (mm)	Constant Term	x_{halo}	H
1×10^{-6}	0.475	5×10^{-2}	0.43	6.7×10^{-4}
5×10^{-7}	0.501	9×10^{-3}	0.44	1.7×10^{-4}
4×10^{-7}	0.516	6×10^{-3}	0.45	1.3×10^{-4}
3×10^{-7}	0.574	2×10^{-6}	0.46	1.0×10^{-4}
2×10^{-7}	0.624	0	0.47	6.0×10^{-5}
1×10^{-7}	NA	0	NA	0

Table VI: Parameters from fitting the transverse beam profiles from different beam gas pressures. The core of the beam has $\sigma = 0.1$ mm and a total of one million particles were tracked.

Additionally the results of these studies are being used to identify ways to control halo formation (better steering algorithms, less beam gas...) in the 12 GeV design and operation.

---

[1] Beam Halo Dynamics, Diagnostics, and Collimation: 29th ICFA Advanced Beam Dynamics Workshop on Beam Halo Dynamics, Diagnostics, and Collimation HALO'03, AIP Conference Proceedings Volume 693.

[2] Studies of Twiss parameters values for a mismatch, result in a β function 50% larger then the design value. This is before any attempt to match the beam. This results in an intrinsic beam size 22% larger then design. A 22% increase in beam size is 110μm for a 0.5mm beam, this is to be compared to the steering allowance of 1mm. This is before the beam has been matched, after the beam has been matched the Twiss parameters returned to the design value. Tech-note in preparation.

[3] A.P. Freyberger, "Large Dynamic Range Beam Profile Measurements" in *DIPAC 2005 Lyon, France*, http://accelconf.web.cern.ch/AccelConf/d05/PAPERS/ITMM04.PDF

[4] R. Servranckx, K. Brown, L. Schachinger, D. Douglas,P. Tenenbaum "Users Guide to the Program DIMAD", http://www.slac.stanford.edu/accel/ilc/codes/dimad/dimad.pdf, July 2004.

[5] M. Borland, "elegant: A Flexible SDDS-Compliant Code for Accelerator Simulation," in *APS LS-287*, presented at ICAP 2000, Darmstadt, Germany

[6] Optim V. Lebedev, "Optim: Computer code for linear and non-linear optics calculations", http://www-bdnew.fnal.gov/pbar/organizationalchart/lebedev/OptiM/optim.htm

[7] I. Reichel, "Study of the Transverse Beam Tails at LEP",CERN-Thesis-98-017.

[8] Geant4, a simulation toolkit, Nuclear Instruments and Methods in Physics Research, A506 (2003) pp 250-303

[9] g4beamline, a "Swiss Army Knife" for Geant4, optimized for simulating beamlines. Muons, Inc corporation, http://www.muonsinc.com

[10] matching studies, tech-note in preparation

[11] hallD 8 degrees beamline, private communication.

[12] Y. Chao, "Evaluation and Optimization of Orbit Correction System Configuration of 12 GeV CEBAF", JLAB-TN-06-015

[13] Y. Chao, "Testing Rationale of 12 GeV Globally Optimized Optics in 6 GeV CEBAF", JLAB-TN-06-014

[14] Leigh Harwood, private communication.

[15] Eduard Pozdeyev , "An estimate of the maximum acceptable strength of field inhomogeneities in Arc 10 dipoles and quadrupoles of the 12 GeV CEBAF Upgrade", JLAB-TN-06-029